Tellus (2007), 59B, 318–325
Printed in Singapore. All rights reserved

TELLUS

CFC-11, $\Delta^{14}C$ and ^{3}H tracers as a means to assess anthropogenic CO_2 concentrations in the ocean

By F. TOURATIER*, L. AZOUZI and C. GOYET, *IMAGES, Université de Perpignan, 52 avenue Paul Alduy, 66860 Perpignan, France*

(Manuscript received 27 June 2006; in final form 8 November 2006)

ABSTRACT

Since anthropogenic CO_2 concentrations in the ocean cannot be measured, it is very difficult to assess the accuracy of the various estimates. Until now, only comparisons among the various approaches and hypotheses have been used to estimate the uncertainties of the results. Here we use three measured anthropogenic tracers (CFC-11, $\Delta^{14}C$ and ^{3}H) to assess the relevance of three estimates of anthropogenic CO_2 distributions based upon very different hypotheses.

In order to focus this work on the correlations among tracers and estimates of anthropogenic CO_2 concentrations in the ocean, we chose as an example the data set from the WOCE I1 cruise (Indian Ocean; 1995), since it included data from the three tracers as well as data of the carbonate/CO_2 properties. This choice further allows us to use the published results of anthropogenic CO_2 concentrations using both the ΔC^* and MIX approaches. Using four properties (total dissolved inorganic carbon, total alkalinity, dissolved oxygen and potential temperature) of this data set, we also estimated the distribution of anthropogenic CO_2 using the recent TrOCA approach.

The results of correlations of anthropogenic CO_2 concentrations with the anthropogenic tracers ^{3}H, CFC-11 and $\Delta^{14}C$, indicate that these correlations are significantly higher when anthropogenic CO_2 is estimated using either the MIX or the TrOCA approaches than using the ΔC^* approach. Based upon these results and the easiness to use the simple TrOCA approach we propose to use this method to unravel the distribution of anthropogenic carbon in the Ocean.

1. Introduction

Since the beginning of industrialization, the carbon dioxide content in the atmosphere increased by ca. 30% (from ∼280 to 370 ppm; Barnola, 1999; Keeling and Whorf, 2000). However, the increase of atmospheric CO_2 is lower than expected. During the 1980's the discharge of CO_2 due to the fossil fuel burning (5.4 ± 0.3 PgC yr^{-1}) was higher than the accumulation of anthropogenic CO_2 in the atmosphere (only 3.3 ± 0.1 PgC yr^{-1}; Sarmiento and Gruber, 2002). According to the latter authors, the difference which amounts to 2.1 ± 0.3 PgC yr^{-1} is taken up by the ocean (1.9 ± 0.6 PgC yr^{-1}) and the biosphere (0.2 ± 0.7 PgC yr^{-1}). The ocean is thus a key reservoir which mitigates the accumulation of anthropogenic CO_2 in the atmosphere. Negative effects are however expected from the accumulation of anthropogenic CO_2 in the ocean, such as the acidification of seawater (Caldeira and Wickett, 2005) and its consequences on marine organisms (Ishimatsu et al., 2005; Nakayama et al., 2005).

In order to quantify the capacity of the ocean to sequester anthropogenic CO_2 and the increase of acidification, the concentration of anthropogenic CO_2 should be accurately known. Since anthropogenic CO_2 cannot be measured, several independent models have been proposed to separate the anthropogenic signal from the bulk of dissolved inorganic carbon (C_T). Two major kinds of models are identified: (1) the ocean circulation models and (2) the back calculation techniques. Examples of OGCMs used in the former type of models are the 2.5-D model of Stocker et al. (1994), the IPSL model (Delecluse, 1994; Madec and Imbard, 1996; Aumont et al., 1999), the MPI model (Maier-Reimer, 1993; Maier-Reimer et al., 1993), the Hadley model (Taylor, 1995) and the Princeton model (Sarmiento et al., 1995; Murnane et al. 1999).

Among models using back calculation techniques, Brewer (1978) and Chen and Millero (1979) were the first to estimate anthropogenic CO_2 from the discrete C_T measurements, taking into account C_T variations due to remineralization and carbonate dissolution. Applications of this kind of model have been performed by several authors, at different locations and with varying levels of details (Chen and Pytkowicz, 1979; Chen, 1982; Papaud and Poisson, 1986; Poisson and Chen, 1987; Chen et al., 1990; Chen, 1993; Goyet and Brewer, 1993; Tsunogai et al., 1993; Chen et al., 1995; Goyet et al., 1998).

In order to attempt to reduce the uncertainties associated with the Brewer and Chen&Millero models (Shiller, 1981; Broecker

*Corresponding author.
e-mail: touratie@univ-perp.fr
DOI: 10.1111/j.1600-0889.2006.00247.x

et al., 1985), Gruber et al. (1996) improved this method by introducing the quasi-conservative tracer C^*. This approach has been used to compute the concentrations of anthropogenic CO_2 throughout the Atlantic Ocean (Gruber et al., 1996; Gruber, 1998) and the Indian Ocean (Sabine et al., 1999). It is based upon the estimate of water masses ages from tracers such as CFC-11, CFC-12, tritium (^{3}H) and helium (^{3}He).

Peng et al. (1998) proposed another kind of approach which is a comparison of C_T measurements between two different time periods in the Indian Ocean. The difference is assumed to reflect the anthropogenic input over the time period. However, high frequency re-sampling would be necessary to apply this technique over a large area since ocean circulation and seasonal changes could counteract the assumption of insignificant change in matter masses during the measurement period.

The following year, Goyet et al. (1999) developed the MIX approach based upon an optimum multi-parameter mixing analysis. Using the single data set from the WOCE I1 section (northern Indian Ocean), Coatanoan et al. (2001) compared the anthropogenic CO_2 estimates computed using independently the MIX and the ΔC^* approaches.

Recently, Waugh et al. (2004) also developed a methodology (the TTD approach) to compute the distribution of anthropogenic CO_2 in the North Atlantic Ocean based upon transit-time distributions estimated from CFCs, ^{3}H and ^{3}He.

The same year, Touratier and Goyet (2004a, b) developed another approach (the TrOCA approach) which uses the quasi-conservative tracer TrOCA (Tracer combining Oxygen, inorganic Carbon and total Alkalinity) and the conservative tracer TrOCA°. It was initially applied to estimate the distribution of anthropogenic CO_2 throughout the Atlantic Ocean. It was then applied to the WOCE I6 section (from South Africa to Antarctica) by Lo Monaco et al. (2005), and to the equatorial Atlantic Ocean by Touratier et al. (2005).

Other recent improvements of ΔC^* approach include those described by Thomas and Ittekot (2001), Thomas et al. (2001) and Perez et al. (2005), while Lo Monaco et al. (2005) improved the Chen and Millero (1979) approach.

In the present context of global change, the scientific community recognizes the need for a large spectrum of independent methodologies to accurately estimate the distribution of anthropogenic CO_2 in the ocean. Well-designed intercomparison exercises are now useful to identify the best methodologies. Several exercises have been done recently (Wanninkhof et al., 1999; Coatanonan et al., 2001; Friis, 2006) or are currently in their implementation phase (CARBOOCEAN project; http://www.carboocean.org/).

Here we show that a combination of three anthropogenic tracers (CFC-11, Δ^{14}C and ^{3}H) provide a powerful tool to improve a simple comparison among estimates of anthropogenic CO_2 distributions based upon different hypotheses, and to assess the realism of the anthropogenic CO_2 distributions.

2. Materials and procedures

2.1. The WOCE I1 data set

Samples were collected from 29 August to 16 October 1995 in the northern Indian Ocean during the WOCE I1 cruise aboard the oceanographic vessel R/V Knorr. A total of 158 stations (Fig. 1) were deployed along three sections located in the Gulf of Aden (section A–B), the Arabian Sea (section C–D) and the Bay of Bengal (section E-F). When applying the TrOCA approach, measurements of potential temperature (θ; °C), dissolved oxygen (O_2; μmol kg^{-1}), total dissolved inorganic carbon (C_T; μmol kg^{-1}) and total alkalinity (A_T; μmol kg^{-1}) are required to estimate the concentration of anthropogenic CO_2 (C_{ant}^{TrOCA}; μmol kg^{-1}). Measured data for θ, O_2, C_T and A_T are available from the CDIAC website (http://cdiac.esd.ornl.gov/), whereas the three anthropogenic tracers ^{3}H (TU), CFC-11 (pmol kg^{-1}) and Δ^{14}C (‰) are available from the WOCE website (http://whpo.ucsd.edu/whpoindian.htm).

2.2. Methods used to estimate the anthropogenic CO_2 along the WOCE I1 sections

Since both the ΔC^* and the MIX approaches used here to estimate the concentration of anthropogenic CO_2 are detailed elsewhere in the literature, just a reminder of their basic equations is given below. Concerning the TrOCA approach, it is described in details since we use Δ^{14}C and CFC-11 tracers to improve the determination of TrOCA^0.

2.2.1. The ΔC^* approach. When applying the method of Gruber et al. (1996), the concentration of anthropogenic CO_2 is calculated from the following equation:

$$C_{ant}^{\Delta C^*} = \Delta C^* - \Delta TCO_2^{diseq}, \quad (1)$$

where ΔC^* is a quasi-conservative tracer based on C_T and ΔTCO_2^{diseq} is a component representing the CO_2 disequilibrium between the pre-industrial atmosphere and the surface ocean.

Sabine et al. (1999) were the first to apply the ΔC^* model to estimate the anthropogenic CO_2 throughout the Indian Ocean using the WOCE and the JGOFS data sets.

2.2.2. The MIX approach. The MIX approach has been developed by Goyet et al. (1999) using the WOCE I1 data set. This method is based upon an optimum multi-parameter mixing analysis from which the mixing coefficients of n water sources (k_j) are deduced. The concentration of anthropogenic CO_2 is then estimated using the following equation:

$$C_{ant}^{MIX} = \sum_{j=1}^{n} k_j \; C_{ANTj} \; F_j(z), \quad (2)$$

where C_{ANTj} is the concentration of anthropogenic CO_2 in the water source j, and $F_j(z)$ are sigmoid functions which add the constraint that anthropogenic CO_2 decreases with increasing distance (and consequently age) from the considered water source.

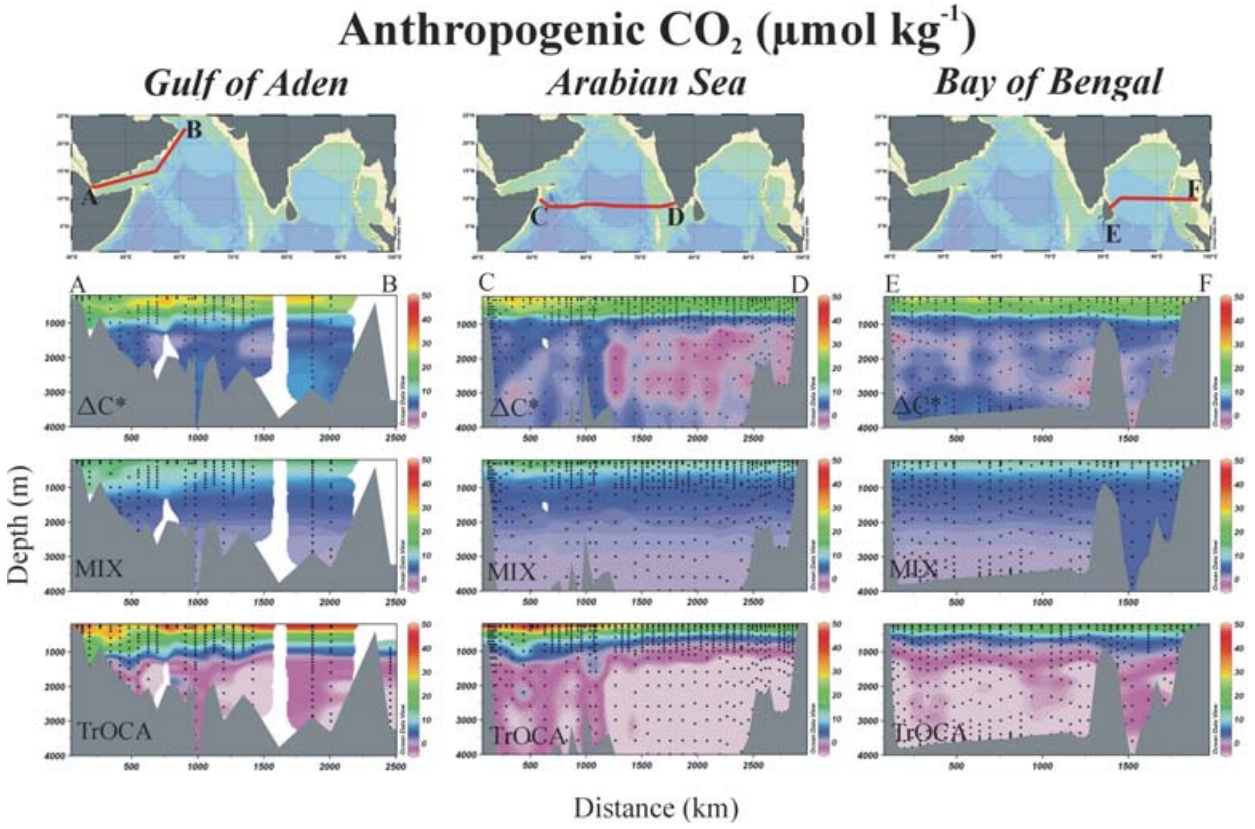

Fig. 1. Distribution of anthropogenic CO_2 (μmol kg^{-1}) estimated with the three approaches (ΔC^*, MIX and TrOCA) and for the three sections of the WOCE I1 cruise. Anthropogenic CO_2 profiles estimated with the MIX and the ΔC^* approaches are from Goyet et al. (1999) and Coatanoan et al. (2001). Sections A–B, C–D and E–F refer to the Gulf of Aden, the Arabian Sea and the Bay of Bengal section, respectively.

2.2.3. The TrOCA approach. The TrOCA tracer is based upon the Redfield equation (eq. 3):

$$(C_{106}H_{263}O_{110}N_{16}P) \; + \; 138\,O_2 \underset{photosynthesis}{\overset{respiration,\ decomposition}{\rightleftharpoons}} 106\,CO_2 \; + \; 16\,NO_3^- \; + \; HPO_4^{2-} + 122\,H_2O \; + \; 18\,H^+. \tag{3}$$

In practice, however, there are some variations on the Redfield coefficients, as shown by several studies in different part of the oceans (Takahashi et al., 1985; Anderson and Sarmiento, 1994; Körtzinger et al., 2001). Using a symbolic notation for the coefficients of the equation (ψ_x), the Redfield equation can be re-written:

$$\left[C_{\left(\psi_{CO_2}\right)}H_{\left(\psi_{HPO_4^{2-}}+2\psi_{H_2O}+\psi_{H^+}\right)}O_{\left(2\psi_{CO_2}+3\psi_{NO_3}+4\psi_{HPO_4^{2-}}+\psi_{H_2O}-2\psi_{O_2}\right)}N_{(\psi_{NO_3})}P_{\left(\psi_{HPO_4^{2-}}\right)}\right] \; + \; \psi_{O_2}O_2.$$
$$\underset{photosynthesis}{\overset{respiration,\ decomposition}{\rightleftharpoons}} \psi_{CO_2}CO_2 \; + \; \psi_{NO_3^-}NO_3^- \; + \; \psi_{HPO_4^{2-}}HPO_4^{2-} \; + \; \psi_{H_2O}H_2O \; + \; \psi_{H^+}\,H^+ \tag{4}$$

At depth, C_T varies according to the respiration and the dissolution of calcium carbonate (eq. 5), the latter process being estimated using A_T (see Brewer, 1978; Goyet and Brewer, 1993).

$$C_T = \frac{\psi_{CO_2}}{\psi_{O_2}}O_2 + \frac{1}{2}\left[A_T + \frac{\left(\psi_{H^+} - \psi_{HPO_4^{2-}}\right)}{\psi_{O_2}}O_2\right]. \tag{5}$$

Rearranging eq. 5, and applying the same rules of construction as Broecker (1974) did for tracers NO or PO, leads to the definition of tracer TrOCA:

$$\mathrm{TrOCA} = O_2 + a\left(C_T - \frac{1}{2}A_T\right),$$

with

$$a = \frac{\psi_{O_2}}{\psi_{CO_2} + \frac{1}{2}\left(\psi_{H^+} - \psi_{HPO_4^{2-}}\right)}. \tag{6}$$

The conservative tracer $TrOCA^0$ is defined as:

$$\mathrm{TrOCA}^0 = O_2^0 + a\left(C_T^0 - \frac{1}{2}A_T^0\right), \tag{7}$$

where $O_2{}^\circ$, $C_T{}^\circ$ and $A_T{}^\circ$ are the natural concentrations of O_2, C_T and A_T. Then the concentration of anthropogenic CO_2 (C_{ant}^{TrOCA}) is estimated from:

$$C_{ant}^{TrOCA} = \frac{TrOCA - TrOCA^0}{a}. \quad (8)$$

This eq. 8 results from eqs. 6 and 7 knowing that A_T is not affected by the increase of atmospheric CO_2 (e.g. Chen and Millero, 1979; Goyet et al., 1999), i.e. $A_T{}^0 = A_T$; and assuming that $O_2{}^\circ \approx O_2$. The latter approximation results from a specific O_2:CO_2 exchange ratio of -1.4 for fossil fuel burning (Keeling and Shertz, 1992) and the relative contributions of O_2 and CO_2 within the atmosphere of $\sim$21 and 0.037%, respectively. The atmospheric CO_2 reservoir is thus $\sim$500 times more sensitive to the anthropogenic pressure than that of O_2, and we assume that large scale distribution of oxygen in the ocean interior is not significantly affected by human activities.

In the original paper (Touratier and Goyet, 2004b), $TrOCA^0$ was computed only as a function of θ. Here we propose an improved equation based on θ and A_T, deduced from $\Delta^{14}C$ and CFC-11 tracers. $TrOCA^0$ is determined using the GLODAP world ocean database (http://cdiac.ornl.gov/oceans/glodap/Glodap_home.htm) which consists of 9618 hydrographic stations collected on 95 cruises since the 1990s.

First, we assume that all sampling points where $\Delta^{14}C$ is lower than $-175‰$ are free of anthropogenic CO_2. This is valid since the approximate age of the corresponding water masses is higher than $\sim$1400 years (Key, 1991; Matsumoto and Key, 2004; Butzin et al., 2005). These water masses are thus much older than those formed since the beginning of the industrial era ($\sim$200 years ago). Most of the selected 1212 sampling points are located primarily in the northern Pacific Ocean at depths where the oldest water masses are usually found (1000–2000 m), and in deep waters of the northern Indian Ocean. Using the associated properties O_2, C_T and A_T, the corresponding $TrOCA^0$ values are computed using Eq. 6.

Second, we computed the partial pressure of CFC-11 (pCFC-11; in pptv) from the measured concentration of CFC-11 (in pmol kg^{-1}), θ and S using the solubility equation of Warner and Weiss (1985). Then we selected the data set associated with the maximum values of pCFC-11 (typically between 262.9 and 271.3 pptv). This selected data set (1445 points) corresponds to the years 1992–1995 when pCFC-11 reached his maximum in the atmosphere (Fig. 2), and consequently in the surface ocean. From these selected data corresponding to the years 1992–1995, $TrOCA^0$ can be estimated from eq. 8 as:

$$TrOCA^0 = TrOCA - aC_{ant92/95}^{TrOCA}$$

with

$$C_{ant92/95}^{TrOCA} = C_T^{p357} - C_T^{p280}, \quad (9)$$

where C_T^{p357} and C_T^{p280} are the computed concentrations of C_T for the period 1992–1995 and the pre-industrial period, since a pCO_2 of 357 μatm is representative of the 1992–1995 period

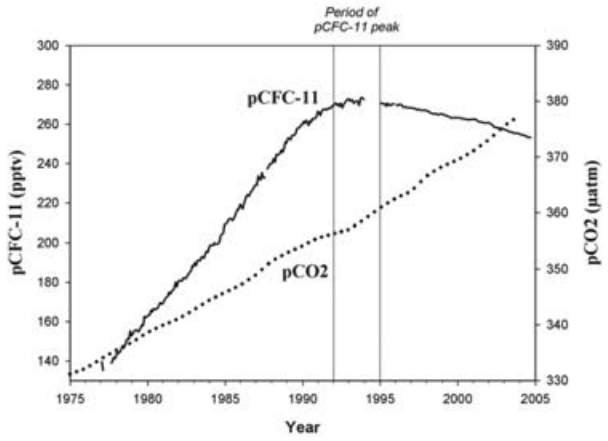

Fig. 2. Time evolution of CFC-11 partial pressure (pCFC-11 in pptv; global mean of pCFC-11 from NOAA/CMDL in Boulder, CO) and CO_2 partial pressure (pCO_2 in μatm; Mauna Loa Observatory, Hawaï) in the atmosphere.

(Fig. 2), and a pCO_2 of 280 μatm is representative of the pre-industrial period. The associated S, θ and A_T properties of the selected samples are also used for the calculation.

Since the value of `a' influences the values of $TrOCA^0$, we computed several sets of $TrOCA^0$ with `a' varying from 1.00 to 1.50. For each set, the $TrOCA^0$ values derived from $\Delta^{14}C$ and pCFC-11 are pulled together and fitted with the following exponential function which best fit the data:

$$TrOCA^0 = TrOCA - a\, C_{ant92/95}^{TrOCA} = e^{\left(b + c\theta + \frac{d}{A_T^2}\right)}. \quad (10)$$

Since $TrOCA^0$ is a conservative property, the 4 parameters are determined by minimizing the fit standard error of Eq. 10. In practice the parameter `a' is the most sensitive for accuracy (see Section 2.2.4 below), and all parameters are determined when the value of `a' corresponds to the minimum of the standard error curve. Thus the optimal set of parameters is the following:

$$\begin{cases} a = 1.279 \pm 7.3 \times 10^{-3} \\ b = 7.511 \pm 5.2 \times 10^{-3} \\ c = -1.087 \times 10^{-2} \pm 2.5 \times 10^{-5} \\ d = -7.81 \times 10^{5} \pm 2.9 \times 10^{4} \end{cases}$$

The concentration of C_{ant}^{TrOCA} is then estimated using eq. 11:

$$C_{ant}^{TrOCA} = \frac{O_2 + 1.279\left[C_T - \frac{1}{2}A_T\right] - e^{\left(7.511 - \left(1.087\times10^{-2}\right)\theta - \frac{7.81\times10^5}{A_T^2}\right)}}{1.279}. \quad (11)$$

2.2.4. Precision of the methods. The precision of the ΔC^* approach is in the order of 10 μmol kg^{-1} (Gruber et al., 1996). Using the WOCE I1 data set, Goyet et al. (1999)

estimated a precision for the MIX approach of 3.7 μmol kg^{-1}. From eq. 11, the uncertainty associated with the $C_{\text{ant}}^{\text{TrOCA}}$ estimate could be computed using the technique of error propagation:

$$\begin{aligned}\delta^2_{C_{\text{ant}}^{\text{TrOCA}}} = &\left\{\left(\frac{\partial C_{\text{ant}}^{\text{TrOCA}}}{\partial C_T}\right)\delta_{C_T}\right\}^2 + \left\{\left(\frac{\partial C_{\text{ant}}^{\text{TrOCA}}}{\partial O_2}\right)\delta_{O_2}\right\}^2 \\ &+ \left\{\left(\frac{\partial C_{\text{ant}}^{\text{TrOCA}}}{\partial A_T}\right)\delta_{A_T}\right\}^2 + \left\{\left(\frac{\partial C_{\text{ant}}^{\text{TrOCA}}}{\partial \theta}\right)\delta_{\theta}\right\}^2 \\ &+ \left\{\left(\frac{\partial C_{\text{ant}}^{\text{TrOCA}}}{\partial a}\right)\delta_{a}\right\}^2 + \left\{\left(\frac{\partial C_{\text{ant}}^{\text{TrOCA}}}{\partial b}\right)\delta_{b}\right\}^2 \\ &+ \left\{\left(\frac{\partial C_{\text{ant}}^{\text{TrOCA}}}{\partial c}\right)\delta_{c}\right\}^2 + \left\{\left(\frac{\partial C_{\text{ant}}^{\text{TrOCA}}}{\partial d}\right)\delta_{d}\right\}^2.\end{aligned} \quad (12)$$

However in practice, the uncertainty for each GLODAP sampling point is estimated after generating 1000 random perturbations in the deltas (δ) of all involved parameters (a, b, c and d) and variables (C_T, O_2, A_T and θ). Assuming $\delta_{C_T} = 2$ μmol kg^{-1}, $\delta_{O_2} = 1$ μmol kg^{-1}, $\delta_{A_T} = 4$ μmol kg^{-1}, $\delta_\theta = 0.01$ °C, $\delta_a = 7.3 \times 10^{-3}$, $\delta_b = 5.2 \times 10^{-3}$, $\delta_c = 2.5 \times 10^{-5}$ and $\delta_d = 2.9 \times 10^4$, then $\delta_{C_{\text{ant}}^{\text{TrOCA}}} = 6.25$ μmol kg^{-1}.

Note that the uncertainty on $C_{\text{ant}}^{\text{TrOCA}}$ due to the uncertainties of variables only is 1.93 μmol kg^{-1}. The uncertainty on $C_{\text{ant}}^{\text{TrOCA}}$ reaches 5.94 μmol kg^{-1} when only the uncertainties of parameters (a to d) are considered. The uncertainty of parameter a alone generates an uncertainty on $C_{\text{ant}}^{\text{TrOCA}}$ of 3.31 μmol kg^{-1}.

3. Results and discussion

3.1. Distribution of anthropogenic CO_2

The distributions of anthropogenic CO_2, as estimated by the three methods (ΔC^*, MIX and TrOCA), are shown in Fig. 1 for the Gulf of Aden, the Arabian Sea and the Bay of Bengal. The results shown in Fig. 1 for the MIX and the ΔC^* approaches were published previously in Goyet et al. (1999) and Coatanoan et al. (2001), respectively.

Whatever the section, the concentrations of anthropogenic CO_2 estimated by the ΔC^* and the TrOCA approaches in the subsurface layer (below 200 metres) are generally higher than those estimated using the MIX approach. This is particularly evident for the Gulf of Aden where $C_{\text{ant}}^{\Delta C^*}$ and $C_{\text{ant}}^{\text{TrOCA}}$ reach 37 and 50 μmol kg^{-1}, respectively (Fig. 1), while $C_{\text{ant}}^{\text{MIX}}$ does not exceed 18 μmol kg^{-1}. All these methods clearly indicate that continental waters are more contaminated than open-sea waters. Results within the mixed layer (0–200 m) are not considered since it is well known that all back calculation techniques are inadequate to estimate anthropogenic CO_2 within the surface layer. This is due to the hypotheses of constant elemental ratios and of a closed system which cannot be respected since there are biological activities and gas transfers across the air–sea interface.

Along the three sections, negative estimates of anthropogenic CO_2 concentrations appear below 1000 m when both the ΔC^* and the TrOCA approaches are used. However the mean of the negative values computed with the TrOCA approach is of -4.6 μmol kg^{-1}, i.e. within the uncertainty of the approach (± 6.25 μmol kg^{-1}).

As mentioned during the description of the TrOCA approach (Section 2.2.4) when using the world Ocean database GLODAP, deep waters (below 1000 m) of the northern Indian Ocean are probably very old (>1200 years; calculation based on the Δ^{14}C; Key, 1991). Even if there are uncertainties associated with the estimate of water mass age, these waters certainly sank long before the beginning of the industrial era. Since the values of TrOCA^0 are defined using such low Δ^{14}C values, slightly negative $C_{\text{ant}}^{\text{TrOCA}}$ may appear. Results of the MIX approach for the Arabian Sea show very little longitudinal variability and results are always positive.

Profiles throughout the Bay of Bengal (Fig. 1) exhibit a regular decrease of the anthropogenic CO_2 concentration with depth when the MIX is applied. According to these results, bottom waters East of 92°E (in the Andaman Sea) are more contaminated by anthropogenic CO_2 than those located west of 92°E. The ΔC^* and the TrOCA approaches do not show such differences in the concentration of anthropogenic CO_2 between the two basins. West of 92°E, in contrast to the other approaches, significant concentrations of anthropogenic CO_2 are estimated in bottom waters from the ΔC^* approach.

Profiles of anthropogenic CO_2 corresponding to each method are shown in Fig. 3. Obvious differences exist in the range of anthropogenic CO_2 estimated by each method. The concentration of anthropogenic CO_2 decreases progressively with depth when either the MIX or the TrOCA approach is applied, whereas the ΔC^* approach generates an abrupt change in the concentration within the 600–800 m depth range.

3.2. Relationships between the three anthropogenic CO_2 estimates

Thereafter, spearman correlations are analysed for depths ranging from 200 m (the mixed layer depth) to 2000 m. Differences exist in the correlations between the three anthropogenic CO_2 estimates (ΔC^*, MIX and TrOCA; see Table 1). The correlation MIX versus TrOCA is relatively higher ($R = 0.95$) than the correlations ΔC^* versus MIX ($R = 0.86$) and ΔC^* versus TrOCA ($R = 0.93$). Despite a large difference in the anthropogenic CO_2 maxima between the TrOCA and the MIX approach ($\sim$50 and 20 μmol kg^{-1}, respectively) the strong correlations suggest that the two methods lead to anthropogenic CO_2 profiles of similar shape (Fig. 3). Profiles computed with the ΔC^* approach are very different in shape due to the abrupt change of concentration in the layer 600–800 m (Fig. 3). This largely explains the lower correlations of the ΔC^* versus MIX and ΔC^* versus TrOCA.

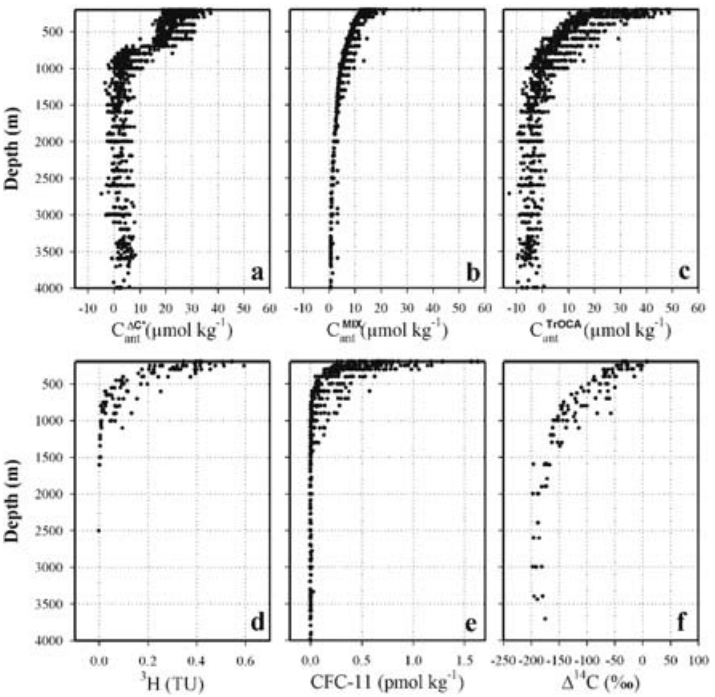

Fig. 3. Vertical distributions of anthropogenic CO_2 estimated with (a) the ΔC^* approach, (b) the MIX approach and (c) the TrOCA approach. For comparison, the vertical distributions of three other anthropogenic tracers are considered: (d) the tritium, (e) the CFC-11 and (f) the $\Delta^{14}C$.

3.3. Relationships between the anthropogenic CO_2 estimates and ^3H, CFC-11 and $\Delta^{14}C$

Here, three different tracers (^{3}H, CFC-11 and Δ^{14}C) are used to assess independently the relevance of the three anthropogenic CO_2 estimates. These tracers have been measured with the associated properties θ, O_2, C_T and A_T. Natural ^{3}H, CFC-11 and Δ^{14}C are present in both the atmosphere and the oceans at very low concentration levels. Anthropogenic levels of ^{3}H and Δ^{14}C however dramatically increased after the atmospheric bomb tests which started in the 1950s, whereas the concentration of anthropogenic CFC-11 in the atmosphere increased since the 1930s, in parallel with the outburst of the industrial activity (England and Maier-Reimer 2001). These tracers are very interesting anthropogenic tracers to study the anthropogenic CO_2 invasion of ocean interior since the temporal evolution of their concentrations in the atmosphere is somewhat similar to that of anthropogenic CO_2. It must be kept in mind however that significant differences exist between these tracers. Tracers Δ^{14}C and ^{3}H have been injected as pulses into the atmosphere during the 1950s, whereas anthropogenic CO_2 has increased progressively since ~130 yr. Moreover, the air–sea equilibration time for Δ^{14}C is ~10 times greater than for anthropogenic CO_2 (Broecker and Peng, 1974). According to England and Maier-Reimer (2001), the penetration of tracer ^{3}H into the ocean is a complex function of numerous factors (e.g. rainfall, moisture, geographic location, river input and origin of air masses). Concerning tracer CFC-11, the sources of emission also differ with those of anthropogenic CO_2, whereas the time of equilibration is ~10 times shorter (Broecker and Peng, 1982). However the distributions of anthropogenic ^{3}H (Fig. 3d), CFC-11 (Fig. 3e) and Δ^{14}C (Fig. 3f) are often assumed to be similar to that of anthropogenic CO_2 in the ocean interior for two main reasons: (1) these tracers have been released initially into the atmosphere, as it is the case for anthropogenic CO_2 and (2) they are conservative (their distribution is not affected by the biology and/or the chemistry), as it is also the case for anthropogenic CO_2 if we consider that it is a minor fraction of the bulk of C_T.

Another point supports the relevance of using these tracers here: they are highly correlated (see Table 1), with the correlation coefficient of ^{3}H versus CFC-11 reaching a value of 0.99.

Correlation coefficients between the measured anthropogenic tracers (^{3}H, CFC-11 and Δ^{14}C) and the three estimates of anthropogenic CO_2 are given in Table 1. All correlations of the measured tracers with MIX and TrOCA are high ($R \geq 0.93$) with the strongest relationship seen for Mix versus Δ^{14}C ($R = 0.98$).

Table 1. Spearman correlations between the four anthropogenic tracers (anthropogenic CO_2, Tritium, CFC-11 Δ^{14}C). The concentration of anthropogenic CO_2 is estimated using three different approaches (ΔC^*, MIX and TrOCA). All coefficients (R) values are significant at the 0.05 level

	ΔC^*	MIX	TrOCA	Tritium	CFC-11
MIX	0.86				
TrOCA	0.93	0.95			
Tritium	0.87	0.97	0.96		
CFC-11	0.87	0.95	0.93	0.99	
Δ^{14}C	0.89	0.98	0.96	0.97	0.97

However, in spite of the fact that the ΔC^* method is based on CFCs data, this approach always has the lower correlation coefficients ($R \leq 0.89$).

4. Conclusions

The results of the Spearman correlations (Table 1) highlight a major difference between the anthropogenic CO_2 profiles estimated from the MIX and the TrOCA approaches (which concentrations decrease smoothly with increasing depth; see Fig. 3), and those estimated from the ΔC^* approach (which show an abrupt gradient in the concentration of anthropogenic CO_2 between 600 and 800 m). Since each of these three methods are based on very different hypotheses, this major difference may indicate that the MIX and the TrOCA approaches are better suited to estimate the distribution of anthropogenic CO_2.

The above observation is further tested using three additional and independent anthropogenic tracers (CFC-11, $\Delta^{14}C$ and ^3H), all available from the WOCE I1 cruise. The distribution of these tracers (Fig. 3) and the results of the correlations (Table 1) illustrate that relationships among these tracers and anthropogenic CO_2 estimated by either the MIX or the TrOCA approach are strong ($R \geq 0.93$). The correlation CFC-11 versus ΔC^* is expected to be better than those of CFC-11 versus MIX ($R = 0.95$) or CFC-11 versus TrOCA ($R = 0.93$) since CFCs play a crucial role for determining the air–sea disequilibria in this method. However, the result indicate that the R value is relatively low ($R = 0.87$; Table 1). This is somewhat surprising since the two variables CFC-11 and $C_{ant}^{\Delta C^*}$ are partially dependant.

The present study indicates that the MIX approach provides the most persuasive distribution of anthropogenic CO_2 and we recommend this approach for regional studies where the distribution of water masses can be clearly defined. However, for large scale and 2- to 3-D modelling studies, the TrOCA approach is best suited since it is very easy to apply from only four known properties (θ, C_T, A_T and O_2) without any other knowledge of the water mass properties.

The utilisation of independent anthropogenic tracers like CFCs, $\Delta^{14}C$ or/and ^3H provide efficient tools of assessment of available techniques to estimate the distribution of anthropogenic CO_2. Given the high number of available approaches (Brewer, 1978; Chen and Millero, 1979; Gruber et al., 1996; Peng et al., 1998; Goyet et al., 1999; Thomas and Ittekot, 2001; Waugh et al., 2004; Touratier and Goyet, 2004b; Lo Monaco et al., 2005; Perez et al., 2005), it would be useful to take advantage of such multi-tracers comparisons to determine the most appropriate anthropogenic CO_2 estimate in each studied area.

5. Acknowledgments

This work was supported by the CARBOOCEAN project (Marine carbon sources and sinks assessment), funded by the European Community. We are very grateful to C. Sabine who provides the results of the ΔC^* approach, and M. Chalard who helped us in the analysis of the results.

References

Anderson, L. A. and Sarmiento, J. L. 1994. Redfield ratios of remineralization determined by nutrient data analysis. *Glob. Biogeochem. Cycles* **8**, 65–80.

Aumont, O., Orr, J., Monfray, P., Madec, G. and Maier-Raimer, E. 1999. Nutrient trapping in the equatorial Pacific: the ocean circulation solution. *Glob. Biogeochem. Cycles* **13**, 351–370.

Barnola, J. M. 1999. Status of the atmospheric CO_2 reconstruction from ice core analyses. *Tellus* **51B**, 151–155.

Brewer, P. G. 1978. Direct observation of the oceanic CO_2 increase. *Geophys. Res. Lett*. **5**, 997–1000.

Broecker, W. S. 1974. "No", a conservative water mass tracer. *Earth Plant. Sci. Lett.* **23**, 100–1007.

Broecker, W. S., and Peng, T.-H. 1974. Gas exchange rates between air and sea. *Tellus* **26**, 21–35.

Broecker, W. S., and Peng, T.-H. 1982. *Tracers in the sea. Eldigio Press, Lamont-Doherty Geological Observatory*. Palisades, NY.

Broecker, W. S., Takahashi, T., and Peng, T.-H. 1985. Reconstruction of past atmospheric CO_2 from the chemistry of the contemporary ocean: an evaluation. *Tech. Rep. TRO 20, U. S. Dep. of Energy*. Washington, D. C.

Butzin, M., Prange, M. and Lohmann, G. 2005. Radiocarbon simulations for the glacial ocean: the effects of wind stress, Southern Ocean sea ice and Heinrich events. *Earth Plant. Sci. Lett.* **235**, 45–61.

Caldeira, K. and Wickett, M. E. 2005. Ocean model predictions of chemistry changes from carbon dioxide emissions to the atmosphere and ocean. *J. Geophys. Res*. **110**, 1–12

Chen, C.-T. A. and Millero, F. J. 1979. Gradual increase of oceanic CO_2. *Nature* **277**, 205–206.

Chen, C.-T. A. and Pytkowicz, R. M. 1979. On the total CO_2-titration alkalinity-oxygen system in the Pacific Ocean. *Nature* **281**, 362–365.

Chen, C.-T. A. 1982. On the distribution of anthropogenic CO_2 in the Atlantic and Southern oceans. *Deep Sea Res*. **29**, 563–580.

Chen, C.-T. A., Jones, E. P. and Lin, K. J. 1990. Wintertime total carbon dioxide measurements in the Norwegian and Greenland Seas. *Deep-Sea Res*. **37**, 1455–1473.

Chen, C.-T. A. 1993. The oceanic anthropogenic CO_2 sink. *Chemosphere* **27**, 1041–1064.

Chen, C.-T. A., Wang, S.-L. and Bychkov, A. S. 1995. Carbonate chemistry of the Sea of Japan. *J. Geophys. Res*. **100**, 13737–13745.

Coatanoan, C., Goyet, C., Gruber, N., Sabine, C. L. and Warner, M. 2001. Comparaison of two approaches to quantify anthropogenic CO_2 in the ocean: results from the northern Indian Ocean. *Global Biogeochem. Cycles* **15**, 11–25.

Delecluse, P. 1994. Modelling the ocean circulation. In: long-term climatic variations. *NATO ASI Ser*. I, **22**, 73–106.

England, M. H. and Maier-Reimer, E. 2001. Using chemical tracers to assess ocean models. *Rev. Geophys*. **39**, 29–70.

Friis, F. 2006. A review of marine anthropogenic CO_2 definitions: introducing a thermodynamic approach based on observations. *Tellus* **56B**, 2–15.

Goyet, C. and Brewer, P. G. 1993. Biochemical properties of the oceanic carbon cycle. In: *Modelling Oceanic Climate Interactions. NATO ASI*

Series, I 11. (edsJ. Willebrand and D. L. T. Anderson). Springer-Verlag, Berlin, Heidelberg, pp. 271–297.

Goyet, C., Adams, R. and Eischeid, G. 1998. Observations of the CO_2 system properties in the tropical Atlantic Ocean. *Mar. Chem*. **60**, 49–61.

Goyet, C., Coatanoan, C., Eischeid, G., Amaoka, T., Okuda, K., and co-authors. 1999. Spatial variation of total CO_2 and total alkalinity in the northern Indian Ocean: A novel approach for the quantification of anthropogenic CO_2 in the seawater. *J. Mar. Res*. **57**, 135–163.

Gruber, N. 1998. Anthropogenic CO_2 in the Atlantic Ocean. *Global Biogeochem. Cycles* **12**, 165–191.

Gruber, N., Sarmiento, J. L. and Stocker, T. F. 1996. An improved method for detecting anthropogenic CO_2 in the oceans. *Global Biogeochem. Cycles* **10**, 809–837.

Ishimatsu, A., Hayashi, M., Lee, K.-S., Kikkawa, T. and Kita, J. 2005. Physiological effects on fishes in a high-CO_2 world. *J. Geophys. Res.* **110**, 1–8.

Keeling, R. F. and Shertz, S. R. 1992. Seasonal and interannual variations in atmospheric oxygen and implications for the global carbon cycle. *Nature* **358**, 723–727.

Keeling, C. D. and Whorf, T. P. 2000. Atmospheric CO_2 records from sites in the SIO air sampling network. In: *Trends: A compendium of data on Global Change*. CDIAC, Oak Ridge National Laboratory, U.S. DOE, Oak Ridge, Tenn., U.S.A.

Key, R. M. 1991. Radiocarbon. Report WHPO 91-1, Volume 3, Part 3.1.3, WHP Office.

Körtzinger, A., Hedges, J. I. and Quay, P. D. 2001. Redfield ratios revisited: removing the biasing effect of anthropogenic CO_2. *Limnol. Oceanogr*. **46**, 964–970.

Lo Monaco, C., Metzl, N., Poisson, A., Brunet, C. and Shauer, B. 2005. Anthropogenic CO2 in the southern ocean: distribution and inventory at the Indian-Atlantic boundary (World Ocean Circulation Experiment line I6). *J. Geophys. Res*. **110**, C06010, doi: 10.1029/2004jc002643.

Lo Monaco, C., Goyet, C., Metzl, N., Poisson, A. and Touratier, F. 2005. Distribution and inventory of anthropogenic CO_2 in the southern ocean: comparison of three data-based methods. *J. Geophys. Res*. **110**, C09S02, doi: 10.1029/2004jc002571.

Madec, G. and Imbard, M. 1996. A global ocean mesh to overcome the North Pole singularity. *Clim. Dyn*. **12**, 381–388.

Maier-Reimer, E. 1993. Geochemical cycles in an ocean general circulation model: preindustrial tracer distributions. *Glob. Biogeochem. Cycles* **7**, 645–677.

Maier-Reimer, E., Mikolajewicz, U. and Hasselmann, K. 1993. Mean circulation of the Hamburg LSG OGCM and its sensitivity to the thermohaline surface forcing. *J. Phys. Oceanogr*. **23**, 731–757.

Matsumoto, K. and Key, M. 2004. Natural radiocarbon distribution in the deep ocean. In: *Global environmental change in the ocean and on land*. (eds M., Shiomi and H. Kawahata). TERRAPUB, Tokyo, 45–58.

Murnane, R. J., Sarmiento, J. L. and Le Quéré, C. 1999. The spatial distribution of air-sea CO2 fluxes and the interhemispheric transport of carbon by the oceans. *Glob. Biogeochem. Cycles*, **13**, 287–306.

Nakayama, N., Peltzer, E. T., Walz, P. and Brewer, P. G. 2005. First results from a controlled deep sea CO_2 perturbation experiment: evidence for rapid equilibration of the oceanic CO_2 system at depth. *J. Geophys. Res*. **110**, 1–8.

Papaud, A. and Poisson, A. 1986. Distribution of dissolved CO2 in the Red Sea and correlation with other geochemical tracers. *J. Mar. Res*., **44**, 385–402.

Peng, T.-H., Wanninkhof, R., Bullister, J. L., Feely, R. A. and Takahashi, T. 1998. Quantification of decadal anthropogenic CO2 uptake in the ocean based on dissolved inorganic carbon measurements. *Nature*, **38**, 560–563.

Pérez, F. F., Vásquez-Rodríguez, M. and Ríos, A. 2005. Cant evaluation through an improved back-calculation equation. First annual CCAR-BOOCEAN meeting, November 2005, Royal Netherlands Academy of Arts and Sciences, Amsterdam, The Netherlands.

Poisson, A. and Chen, C.-T. A. 1987. Why is there little anthropogenic CO_2 in the Antarctic Bottom Water? *Deep Sea Res. A* **34**, 1255–1275.

Sabine, C. L., Key, R. M., Johnson, K. M., Millero, F. J., Poisson, A., and co-authors. 1999. Anthropogenic CO_2 inventory of the Indian Ocean. *Global Biogeochem. Cycles* **13**, 179–198.

Sarmiento, J. L. and Gruber, N. 2002. Sinks for anthropogenic carbon. *Phys. Today* **55**, 30–36.

Sarmiento, J. L., Murnane, R. and Le Quéré, C. 1995. Air-sea CO_2 transfer and the carbon budget of the North Atlantic. *Philos. Trans. R. Soc. London, B* **348**, 211–219.

Shiller, A. M. 1981. Calculating the oceanic CO_2 increase: a need for caution. *J. Geophys. Res*. **86**, 11083–11088.

Stocker, T. F., Broecker, W. S. and Wright, D. G. 1994. Carbon uptake experiments with a zonally averaged global circulation model. *Tellus* **46B**, 103–122.

Takahashi, T., Broecker, W. S. and Langer, S. 1985. Redfield ratio based on chemical data from isopycnal surfaces. *J. Geophys. Res*. **90**, 6907–6924.

Taylor, N. K., 1995. Seasonal uptake of anthropogenic CO_2 in an ocean general circulation model. *Tellus* **47B**, 145–169.

Thomas, H., England, M. and Ittekot, V. 2001. An off-line 3D model of anthropogenic CO_2 uptake by the oceans. *Geophys. Res. Lett.* **28**, 547–550.

Thomas, H. and Ittekot, V. 2001. Determination of anthropogenic CO_2 in the North Atlantic Ocean using water mass ages and CO_2 equilibrium chemistry. *J. Mar. Syst*. **27**, 325–336.

Touratier, F. and Goyet, C. 2004a. Definition, properties, and Atlantic distribution of the new tracer TrOCA. *J. Mar. Syst*. **46**, 169–179.

Touratier, F. and Goyet, C. 2004b. Applying the new TrOCA approach to assess the distribution of anthropogenic CO_2 in the Atlantic Ocean. *J. Mar. Syst*. **46**, 181–197.

Touratier, F., Goyet, C., Coatanoan, C. and Andrié, C. 2005. Assessment of anthropogenic CO2 distribution in the tropical Atlantic Ocean. *Deep-Sea Res., part I* **52**, 2275–2284.

Tsunogai, S., Ono, T. and Watanabe, S. 1993. Increase in total carbonate in the Western North Pacific water and a hypothesis on the missing sink of anthropogenic carbon. *J. Oceanogr*. **49**, 305–315.

Wanninkhof, R., Doney, S. C., Peng, T.-H., Bullister, J. L., Lee, K., and co-authors. 1999. Comparison of methods to determine the anthropogenic CO_2 invasion into the Atlantic Ocean. *Tellus* **51B**, 511–530.

Warner, M. and Weiss, R. 1985. Solubilities of chorofluorocarbons 11 and 12 in water and seawater. *Deep-Sea Res*. **32**, 1485–1497.

Waugh, D. W., Haine, T. W. N. and Hall, T. M. 2004. Transport times and anthropogenic carbon in the subpolar north Atlantic Ocean. *Deep Sea Res., I* **51**, 1475–1491.